1 **Effects of input data aggregation on simulated crop yields**

2 **in temperate and Mediterranean climates**

3

4 Ganga Ram Maharjan[a*], Holger Hoffmann[a], Heidi Webber[a,i], Amit Kumar Srivastava[a], Lutz

5 Weihermüller[b], Ana Villa[c], Elsa Coucheney[c], Elisabet Lewan[c], Giacomo Trombi[d], Marco

6 Moriondo[d], Marco Bindi[e], Balazs Grosz[f], Rene Dechow[f], Mathias Kuhnert[g], Luca Doro[h],

7 Kurt-Christian Kersebaum[i], Tommaso Stella[i], Xenia Specka[i],Claas Nendel[i], Julie Constantin[j],

8 Hélène Raynal[k], Frank Ewert[a,i], Thomas Gaiser[a]

9 [a] Crop Science Group, INRES, University of Bonn, Germany

10 [b] Agrosphere Institute (IBG-3), Forschungszentrum Jülich GmbH, Jülich, Germany

11 [c] Department of Soil and Environment, Swedish University of Agricultural Sciences, Uppsala, Sweden

12 [d] Department of Agri-Food Production and Environmental Science (DISPAA), University of Florence, Italy

13 [e] CNR-Ibimet, Florence, Italy

14 [f] Thünen-Institute of Climate-Smart-Agriculture, Braunschweig, Germany

15 [g] Institute of Biological and Environmental Sciences, University of Aberdeen, Aberdeen, Scotland, UK

16 [h] Desertification Research Centre, University of Sarrari,Viale Italia, Sassari, Italy

17 [i] Leibniz Centre for Agricultural Landscape Research (ZALF), Müncheberg, Germany

18 [j] AGIR, Université de Toulouse, INRA, Castanet-Tolosan, France

19 [k] MIAT, Université de Toulouse, INRA, Castanet-Tolosan, France

20 * Corresponding author. Present address: YARA- Crop Nutrition Research and Development, Hanninghof 35,

21 48249 Dülmen, Germany: Ganga Ram Maharjan, gmaharja@uni-bonn.de, ganga.ram.maharjan@yara.com,

22 mhjgangaram@gmail.com

23

24

Abstract

26 Soil-crop models are used to simulate ecological processes from the field to the regional

27 scale. Main inputs are soil and climate data in order to simulate model response variables such

28 as crop yield. We investigate the effect of changing the resolution of input data on simulated

29 crop yields at a regional scale using up to ten dynamic crop models. For these models we

30 compared the effects of spatial input data aggregation for wheat and maize yield of two

31 regions with contrasting climate conditions (1) Tuscany (Italy, Mediterranean climate) and (2)

32 North Rhine Westphalia (NRW, Germany, temperate climate). Soil and climate data of 1 km

33 resolution were aggregated to resolutions of 10, 25, 50, and 100 km by selecting the dominant

34 soil class (and corresponding soil properties) and by arithmetic averaging, respectively.

35 Differences in yield simulated at coarser resolutions from the yields simulated at 1 km

36 resolution were calculated to quantify the effect of the aggregation of the input data (soil and

37 climate data) on simulation results.

38 The mean yield difference (bias) at the regional level was positive due to the upscaling of

39 productive dominant soil(s) to coarser resolution. In both regions and for both crops,

40 aggregation effects (i.e. errors in simulation of crop yields at coarser spatial resolution) due to

41 the combined aggregation of soil and climate input data increased with decreasing resolution,

42 whereby the aggregation error for Tuscany was larger than for North Rhine Westphalia

43 (NRW). The average absolute percentage yield differences between grid cell yields at the

44 coarsest resolution (100 km) compared to the finest resolution (1 km) were by about 20 to

45 30% for Tuscany and less than 15 and 20% for NRW for winter wheat and silage maize,

46 respectively.

47 In the Mediterranean area, the prediction errors of the simulated yields could reach up to 60 %

48 when looking at individual crop model simulations. Additionally, aggregating soil data caused

49 larger aggregation errors in both regions than aggregating climate data.

50 Those results suggest that a higher spatial resolution of climate and especially of soil data

51 input are necessary in Mediterranean areas than in temperate humid regions of central Europe

52 in order to predict reliable regional yield estimations with crop models.

53 For generalization of these outcomes, further investigations in other sub-humid or semi-arid

54 regions will be necessary.

55 **Keywords: Data resolution, Scale, Modelling, Regional yield, Climate, Soil**

1. Introduction

57 Crop models were developed based on the understanding and conceptualisation of the effects

58 of agro-climatic conditions on field processes (e.g. soil water movement, nutrient cycle, root

59 water and nutrient uptake). They are applied to simulate crop yield under different agro-

60 climatic and management conditions and to assess climate change impacts on crop yield. The

61 agro-climatic conditions in the field along with crop-management practices are represented by

62 measured soil and climate data, whereby these soil and climate data are the main inputs for

63 crop models that drive the processes implemented in the model. Most crop growth models

64 were developed at the plot or field scale (F. Ewert et al., 2015), where the input data can be

65 measured to initialize and drive the models.

66 Crop models have been generally validated and applied for multiple locations at the plot or

67 field scale (Hansen et al., 2012; Liang et al., 2016; Singh et al., 2013). They can moreover be

68 applied for multiple grid cells of different resolutions to cover the entire area of interest

69 (region to country level). In that case, the spatial variation within the area is defined by

70 different characterization of the grid cells in terms of agro-climatic conditions (such as soil

71 and climate input data) representative of the area covered by the grid. Therefore, these models

72 are run beyond the plot or field scales, where they have been developed at, to predict yields at

73 regional to global scales with various grid resolutions using spatially aggregated input data

74 are were used (Rosenzweig et al., 2014; Rosenzweig and Iglesias, 1998; Rosenzweig and

75 Parry, 1994). For example, crop models are applied using climate change data generated by

76 global circulation models (GCMs) at a scale of e.g. half degree (~50 to 50 km) to assess

77 climate change impacts on crops and the environment (Donatelli et al., 2015) and in order to

78 design comprehensive adaptation strategies such as optimization of sowing date from regional

79 to global scales. When crop models are applied at these large scales, input data (such as soil

80 or climate data) are estimated from smaller scale measurements by data aggregation to the

81 resolution of the grid-cell simulation. The aggregation of input data from finer resolution to

82 coarser resolution inevitably will lead to losses of spatial variability of the dataset, whereby

83 the extent of information loss greatly depends on the aggregation methods (Ewert et al.,

84 2011).

85 Climate input data from two relatively small regions in Northern and Central Europe

86 aggregated to different resolutions was used to run a range of crop models in Angulo et al.

87 (2013) in order to study the characteristics and distribution of the response variable (i.e., crop

88 yield) as a result of the input data aggregation (climate data). Furthermore, soil data at

89 different resolutions were used to simulate crop yield and analyze yield distribution from two

90 contrasting sites in Angulo et al. (2014). These studies showed that the impact of input data

91 (soil and climate respectively) aggregation on simulated yield distribution were not different

92 within models despite that the simulated spatial yield distributions were different for the

93 various models. The authors proposed thus to use a multi-model ensemble approach (i.e.,

94 average of the output of all models) to analyze input data aggregation impact on regional crop

95 yield simulation. A multi-model ensemble approach was also used by Zhao et al. (2015a) who

96 quantified the climate data aggregation error for regional simulations of several model output

97 variables such as yield, evapotranspiration, and water use efficiency in North Rhine-

98 Westphalia (NRW) in Central Europe. In the latter study, climatic data were aggregated at

99   different resolutions (10, 25, 50, and 100 km). They found that climate data aggregation error

100   was highest for simulated crop yield compared to crop evapotranspiration or water use

101   efficiency, but was below 10% in all cases. In the same region, the characteristics (inter-

102   annual variability and spatial variance) of climatic data aggregated to coarser resolution were

103   compared to the simulated regional mean crop yield (winter wheat and silage maize) across

104   various crop models and years, whereby the bias was up to 0.2 t ha^{-1} (< 3 %) due to the

105   aggregation of climate data (Hoffmann et al., 2015). The aggregation error for simulated crop

106   yield was significantly increasing for decreasing resolution of the climate data. The

107   application of simultaneous aggregation of soil and climate data to simulate regional crop

108   yield by different crop models were further investigated by Hoffmann et al. (2016). The

109   results showed, that the aggregation errors were amplified with decreasing resolution of soil

110   and climate data input compared to the aggregation error made by aggregating only one input

111   variable.

112   The study of the aggregation effects of soil and climate data on regional crop yield

113   simulations has so far been focused only on temperate, humid region, namely North-Rhine

114   Westphalia (NRW) in Germany (Hoffmann et al., 2017, 2016; Zhao et al., 2015a) or a boreal

115   region (Angulo et al., 2014, 2013) and no such study has been performed in a Mediterranean

116   climate where drier climatic conditions may increase the effect of climate data aggregation.

117   Additionally, no study has been reported so far to compare the aggregation effect between

118   regions with different soil and climatic conditions. In general, the climate in the

119   Mediterranean region is characterized by higher average air temperature during the crop

120   growing season compared to temperate regions and less precipitation either at the end of the

121   growing season in the case of winter crops, or during the growing season in the case of spring

122   crops. In addition, the soils in the Mediterranean region selected show higher spatial

123   variability with more soils having lower available water capacity due to either coarser soil

124   texture or lower soil depth with higher gravel or stone content. Therefore, periods of water

125   shortage for rainfed crops are more frequent. Under water-limited production conditions, the

126   spatial aggregation of soil type in combination with aggregation of climate variables, is

127   expected to have a stronger impact on simulated crop yield compared to temperate, humid

128   regions.

129   Therefore, this study compares aggregation effects of soil and climate data on regional yield

130   simulation for two contrasting climatic regions for water-limited production conditions based

131   on the hypotheses that (1) input data aggregation affects regional yield simulations more in

132   Mediterranean than in temperate region and (2) input data aggregation error is higher for

133   spring crops (silage maize) compared to winter crops (winter wheat).

2   Material and Methods

2.1   Study regions

136   The aggregation effects of input data (soil and climate) on crop yield simulations were

137   compared between a region under temperate, humid climate conditions North Rhine

138   Westphalia (NRW, 51° 46' 4.1" N and 7° 26' 38.4" E, Germany) and a region under

139   Mediterranean climate conditions, Tuscany (TUS, 43° 41' 14.1 " N and 10° 29' 10.3" E ,

140   Italy). Figure 1 presents the geographical location of the study regions. A summary of the

141   main climatic conditions for these two study sites are presented in Table 1.

142   **[Table 1 Here]**

143   The long-term annual means of selected climatic variables were calculated based on the

144   respective climate data from 1995 to 2011. The annual mean temperature for NRW and TUS

145   are 9.6 º C and 16.1 º C, respectively. The annual mean precipitation sums are 821 mm y^{-1} for

146   NRW and 949.4 mm y^{-1} Tuscany.

147   **[Figure 1 Here]**

148   ## 2.2 Preparation of model input data

149   *2.2.1   Soil data*

150   • NRW

151   The soil data at 1 km resolution for NRW, Germany was originally already aggregated by

152   dominant soil type from approximately 300 m resolution to grid cells of 1 km resolution

153   (Hoffmann et al., 2016). The soil data source for NRW and the methods to derive several soil

154   properties including topsoil organic carbon, soil texture, soil bulk density, and soil albedo are

155   explained in Hoffmann et al, (2016). In a second step the soil data at 1 km resolution was

156   aggregated to coarser resolution by dominant soil type from the 1 km resolution to 10, 25, 50,

157   100 km as well as to a NRW mean (S_{NRW}). The results of the soil data aggregated from 1 km

158   resolution to 100 km resolution for NRW is shown in Fig. 2. The dominant soil type for NRW

159   (S_{NRW}) was a Cambisol.

160   **[Figure 2 Here]**

161   • Tuscany

162   The soil distribution including soil physical and chemical properties were obtained from the

163   data base of Gardin and Vinci (2006). The database contains soil layer-wise information about

164   soil layer thickness, soil texture, gravel and soil organic carbon content. Additional soil

165   properties for each layer (such as soil hydraulic properties) required as input to different crop

166   models were prepared based on soil texture and gravel content information using pedotransfer

167   functions (PTF). In Tuscany, information on soil classification at the soil order level was not

168   available. Therefore, the dominant soil texture in the topsoil at the resolution of 1 km was

169   used to aggregate the soil properties to the resolution of coarser grids (10 – 100 km). The soil

170   data at a coarser resolution of 10, 25, 50, and 100 km were prepared by selecting the dominant

171   soil texture among the 1 km soil grids (Fig. 3).

172   **[Figure 3 Here]**

173   The dominant soil type aggregated at the regional level for Tuscany the dominant soil texture

174   class is loam. The associated soil properties for dominant soils at the regional level such as

175   soil depth, bulk density, wilting point, and field capacity are presented in the supplementary

176   material (Table S1).

177   The variability of soil properties of top soil layer for NRW and TUS at 1 km resolution is

178   shown in Table 2 and the properties for other soil layers are presented in the supplementary

179   material (Table S2). The soil database with similar soil properties among others at the

180   different level of aggregation were used as soil input data to the crop models used in the study

181   presented.

182   The soil depth of the most dominant soil in NRW is about 2.3 m (range 0.1 - 2.3 m for

183   different soil layers in 1 km grid cells), while for Tuscany it is only 1.36 m (range in 0.18 -

184   1.5 m for different soil layers in 1 km grid cells). The field capacity of the first soil layer for

185   the dominant soils are 0.36 and 0.23 m^3 m^{-3} for NRW and Tuscany, respectively. Other soil

186   parameters required to simulate the crop yields are provided in Hoffmann et al. (2016) mainly

187   for NRW region and are shown in the supplementary material (Table S2).

188   **[Table 2 Here]**

189   *2.2.2   Climate data*

190   • NRW

191   The climate data set for NRW at 1 km resolution include daily time series of minimum, mean

192   and maximum air temperature, precipitation, global radiation, wind speed, and relative

193   humidity for the period 1982 to 2011 and was established by interpolation of measured

194   climate variables at 280 weather stations provided by the German Meteorological Services

195   (DWD). All climate variables were aggregated to coarser resolutions from 1 km resolution

196   data by arithmetic averaging. The climate data source and the aggregation process to coarser

197   resolution for NRW are explained in detail in Hoffmann et al. (2016).

198   • Tuscany

199   The daily meteorological data for Tuscany at 1 km resolution from 1995 to 2013 were

200   provided by the Lamma Consortium of Tuscany Region (http://www.lamma.rete.toscana.it/)

201   This dataset includes gridded daily records of minimum, mean and maximum temperature,

202   precipitation, solar radiation, wind speed and relative humidity (about 22,000 grids cells over

203   Tuscany region), which were calculated from the local meteorological network. In particular,

204   daily maximum and minimum temperatures and total daily-cumulated precipitation, collected

205   from 94 and 159 stations, were interpolated according to the DAYMET procedure (Thornton

206   et al., 1997) to produce the relevant daily digital maps as described in Chiesi et al. (2007).

207   These maps were in turn used as input of the MT-CLIM procedure to produce additional daily

208   maps of solar radiation based on the algorithm presented in Thornton et al. (2000), which was

209   specifically calibrated for the Tuscany region (calibration not published). Relative humidity

210   was calculated by using daily minimum and mean air temperature as explain in Allen et al.

211   (1998). Daily data of wind speed at a height of 2 meters were obtained by interpolating the

212   data from 45 weather stations using a nearest neighbour approach.

213   The meteorological data at 1 km resolution were aggregated similar to the approach applied

214   on NRW to coarser resolution of 10, 25, 50, and 100 km by averaging all grid cells at 1 km

215   included within the respective coarser resolution. The spatial variability of average minimum,

216   mean, and maximum temperature for the period from 1995 to 2013 aggregated across

217   resolutions is shown in Fig 4.

218   The daily climate variables for each year during the growing period of the respective crop

219   where averaged from 1995 to 2011 and are shown in Table 3. The mean temperature during

220   the growing season for silage maize in NRW and Tuscany are respectively 16 and 22°C, while

221 the average of mean temperature during the growing period of wheat are 8°C for NRW and

222 12°C for Tuscany. The sum of precipitation during growing season of maize in NRW and

223 Tuscany are similar with the approximate value of 350 mm, while the precipitation sum

224 during growing season of winter wheat in NRW is about 632 and 591 mm for Tuscany. The

225 climate water balance (cwb: ET0−Precipitation, mm) for respective crop growing season and

226 regions is higher for Tuscany than for NRW. The summary statistic of the climatic variables

227 for each region for the respective crop during growing period is presented in Table 3 and the

228 soil properties of the dominant soil type in each region is presented in supplementary

229 material(Table S2).

230 **[Figure 4 Here]**

231 **[Table 3 Here]**

232 **2.3 Model setup**

233 The model ensemble consisted of a total of nine field scale crop models (AgroC, CENTURY,

234 CoupModel, DailyDayCent, EPIC, HERMES, MONICA, SIMPLACE<LINTUL5;SLIM>,

235 STICS), which have been frequently used in climate change impact studies at field to regional

236 scale (Table 4). The respective abbreviations of the models in figures tables are AGRC,

237 CENT, COUP, DayC, EPIC, HERM, MONI, LINT, and STIC. All models were run for both

238 crops (wheat and maize) except COUP, which was only run for wheat. The model runs were

239 constrained by the climate and soil properties as explained in 2.2.1 and 2.2.2 and management

240 rules (see below). In NRW all models were run constraining the maximum root depth to the

241 maximum soil depth (unrestricted root growth) and for Tuscany CENT, DayC, EPIC, LINT,

242 and CENT were run for the same rooting conditions.

243

244 **[Table 4 Here]**

245   Aggregated soil, climate, and crop management data were used for the crop model ensemble

246   to simulate the yield of silage maize and winter wheat. The crop management data with

247   respect to tillage, sowing, and fertilizer application (timing and amount) were fixed for both

248   regions, while the date of harvest for each crop was either simulated or observed harvest dates

249   were used depending on the requirements of the individual models. The detailed crop

250   management data for winter wheat and silage maize in the two regions are shown in Table 5

251   and 6.

252   **[Table 5 Here]**

253   **[Table 6 Here]**

254   The crop models were calibrated at 1 km resolution grid cells by using one typical sowing and

255   one typical harvest date for each crop to match the regional average of observed yields for

256   NRW and Tuscany. The calibration procedure for NRW is further explained in Hoffmann et

257   al., (2016). The grid cells in the respective resolutions are used as simulation points for the

258   models. For example, 1 km resolution of Tuscany consists of 22,000 grids cells and each grid

259   cell is considered as simulation point for yield simulation at 1 km resolution. The yield for

260   winter wheat refers to grain yield, while for the silage maize it refers to the aboveground

261   biomass. Then, all crop models were run for respective crops and different combinations of

262   soil and climate data resolutions as listed in Table 7.

263   **[Table 7 Here]**

264   The combination of input data at different aggregation levels is abbreviated as $S_y x C_z$ (where

265   S_y is the soil data at resolution y and C_z is the climate data at resolution z). Altogether, 15

266   combinations of spatial resolutions of soil and climate input data were used to simulate silage

267   maize and winter wheat for both regions. The modelled output i.e. yield from each individual

268   crop model was summarized for each soil and climate combination to calculate the model

269   ensemble mean and the impacts of soil and climate data aggregation were further analyzed for

270   the simulation results based on this model ensemble mean. The general modelling framework

271   used in this study is presented in Fig. 5.

272   **[Figure 5 Here]**

273   **2.4   Calculation of the aggregation errors**

274   In general, the aggregation errors were calculated as the differences in model output at a given

275   resolution (e.g., 10, 25, 50, 100, Tus or NRW) with respect to the model outputs generated at

276   the highest resolution of 1 km. The error indicators were calculated from the following

277   equations. The effects of aggregation of soil and climate input data on the yield simulations of

278   the model ensemble mean are quantified for each spatial resolution. Equation 1 quantifies the

279   aggregation error relative to the grid cells i.e. pixel level of the finest 1 km resolution, while

280   the other equations quantify the aggregation error at the regional level (average of all N grid

281   cells at 1 km resolution).

282    $AbsPD_j = \left(\dfrac{|YC_j - YF_j|}{YF_j} \right) * 100$ (1)

283   where, $AbsPD_j$ is the absolute percentage yield difference in simulated yield relative to

284   gridcell j, with YF_j is the simulated yield of the respective grid cell j at 1 km resolution and

285   YC_j is the simulated yield in the grid of a coarser resolution that includes grid cell j.

286   The mean difference at the regional scale (MD) is then calculated as the average of the

287   difference between the yield YC_i simulated at coarser resolution disaggregated to 1 km

288   resolution and corresponding to the jth grid cell and the yield YF_j simulated in grid cell j of 1

289   km resolution:

290 $$MD = N^{-1} * \left(\sum_{j=1}^{N} YC_j - YF_j \right) \qquad (2)$$

291 The mean absolute difference (AMD) is the equivalent to the mean difference (MD) except

292 that the absolute value of the yield differences between coarser resolution and the 1 km

293 resolution is used:

294

295 $$AMD = N^{-1} * \left(\sum_{j=1}^{N} |YC_j - YF_j| \right) \qquad (3)$$

296 $AvgYF$ is the average yield at 1 km resolution, where N is the number of grid cells at 1 km

297 resolution, and rAAD is the average absolute yield deviation normalized to the average yield

298 at 1 km resolution.

299 $$AvgYF = N^{-1} * \left(\sum_{j=1}^{N} YF_j \right) \qquad (4)$$

300 $$rAAD = \frac{N^{-1} * \left(\sum_{j=1}^{N} |YC_j - YF_j| \right) * 100}{AvgYF} \qquad (5)$$

301

3 Results

3.1 Spatial pattern of crop yield simulations in NRW and Tuscany

304 *3.1.1 Silage maize yield simulation in NRW and Tuscany*

305 The ensemble mean for silage maize across all crop models simulated for different

306 combinations of aggregated soil and climate data under water limited conditions shows a

307 relatively higher silage maize yield simulated for NRW (Fig. 6A) as compared to Tuscany

308 (Fig. 6B). Additionally, the spatial variability of silage maize yields are highest when both

309 soil and climate input data at the finest resolution (1 km) were used (S_1xC_1 in NRW and

310 Tuscany). For both regions, only small changes in the spatial yield patterns are detectable,

311 when the finest soil input data resolution (S_1 = soil at 1 km) is combined with average climate

312 input data over the entire region (C_{NRW} or C_{Tus}) (Fig. 6, 1stcolumn for each panel i.e. S_1xC_{NRW}

313 and S_1xC_{TUS}). On the other hand, combining dominant soil conditions (S_{NRW} or S_{TUS}) with

314 high resolution climate data (C_1 = climate at 1 km) leads to pronounced differences in the

315 predicted silage maize yield compared to the finest resolution S_1xC_1. The overall range of

316 silage maize yield for NRW is from 10 to 18 t ha^{-1}, while for Tuscany it is from 5 to 18 t ha^{-1}.

317 **[Figure 6 Here]**

318 *3.1.2   Winter wheat simulation in NRW and Tuscany*

319 The average crop yields for winter wheat in NRW are much higher than in Tuscany regardless

320 of the soil-climate input data combination (Fig. 7). Yield for winter wheat in NRW ranges

321 from 4 to 10 t ha^{-1} while for Tuscany it is between 0 and 6 t ha^{-1}. The spatial variability of the

322 ensemble mean yield for (winter) wheat across all models is similar to the variability of the

323 ensemble mean of silage maize yield. In both NRW and Tuscany, the spatial variability of the

324 winter wheat yield is highest when the finest resolution of climate and soil input (S_1xC_1) is

325 used. In Tuscany, the spatial variability of simulated winter wheat yields using the finest

326 resolution of soil and climate input data (S_1xC_1) is comparable to the spatial variability of

327 yields simulated with the combination of finest soil resolution and average regional climate

328 (S_1xC_{TUS}) that exhibit slightly higher values in the northern part of the region. The yield

329 pattern in which the finest resolutions of soil and climate input is used (S_1xC_1 i.e, Fig. 7 1st

330 column of panel B) is comparable with yields produced with the finest climate resolution and

331 the dominant soil type ($S_{TUS}xC_1$ i.e, Fig. 7, 1st column of Panel B). This is in contrast with the

332   spatial variability of winter wheat yields in NRW, where the simulated yields based on the

333   combination of finest climate input resolution with the dominant soil type exhibited a much

334   lower spatial variability as compared to the yield simulated with the highest resolution of both

335   soil and climate input (S_1xC_1 i.e,Fig. 7, 1st column in panel A).

336   **[Figure 7 Here]**

337   Thus, yield simulations for silage maize and winter wheat at finest resolution of soil and

338   climate input at 1 km resolution (S_1xC_1 i.e. Fig. 6 and 7) have the highest spatial variability

339   compared to all other soil and climate input data combinations. With aggregation of soil and

340   climate input data the spatial variability of simulated crop yields decreases (Fig. 6 and 7).

341   However, in the case of winter wheat, when only climate input data is aggregated and

342   combined with the dominant soil type (3rd row, Fig. 7) the spatial variability of simulated

343   yields is much lower in all resolutions. Thus, the aggregation of climate input data has less

344   impact on the spatial variability of simulated wheat yields under water limited conditions than

345   the simultaneous aggregation of soil and climate for both regions.

346   **3.2   Aggregation effects on simulated crop yields**

347   *3.2.1   Aggregation effect on silage maize yield simulations in NRW and Tuscany*

348   In a next step, the aggregation errors were calculated based on Eq. 1-5 for the different

349   regions and combinations of aggregation. Hereby, the finest resolution (S_1xC_1) was always

350   chosen as the reference simulation in each region. The difference of crop yields when

351   simulated at a coarser resolution of soil and climate input compared to the finest resolution at

352   1 km (S_1xC_1) is considered as the effect of input data aggregation on yield simulations. The

353   magnitude of yield differences for silage maize ranged from -6 to 6 t ha^{-1} (Fig. 8) for both

354   regions. In general, the average bias in silage maize yield (MD) due to input data aggregation

355   was always positive, except for the combined aggregation of soil and climate variables in

356   Tuscany ($S_{10}xC_{10}$, $S_{25}xC_{25}$, $S_{50}xC_{50}$ respective MDs are -0.07,-0.56 and -0.17 Fig. 8 Tuscany

357   1st row). For silage maize simultaneous aggregation of soil and climate to coarser resolution

358   of 50 and 100 km caused lower simulated yield in the North-East of NRW compared to the

359   reference resolution (1 km) as indicated by negative yield differences, while higher yields

360   with positive yield difference are observed towards the southern part (Fig. 8, panel A: $S_{50}xC_{50}$

361   and $S_{100}xC_{100}$). A similar pattern can be distinguished when aggregating soil input data to 50

362   and 100 km combined with an average regional climate (Fig. 8, panel A: $S_{50}xC_{NRW}$ and

363    $S_{100}xC_{NRW}$). The combination of an average regional climate for NRW with the soil input data

364   at 1 km resolution has almost no yield difference with respect to the simulated maize yields of

365   the reference resolution (Fig. 8, panel A: S_1xC_{NRW}). The spatial patterns of yield differences

366   for other combinations (Fig. 8, panel A: from $S_{10}xC_{NRW}$ to $S_{100}xC_{NRW}$, 2nd row) are similar to

367   the pattern of yield differences that are observed with the simultaneous aggregation of soil

368   and climate data (Fig. 8, panel A: from $S_{10}xC_{10}$ to $S_{100}xC_{100}$).

369   A similar observation can be made for the spatial patterns of yield differences in Tuscany for

370   maize under water-limited conditions (Fig. 8, panel B). With decreasing resolution of soil and

371   climate input data, the yield differences are positive towards the northern part and negative

372   towards the southern part of Tuscany (Fig. 8, panel B: $S_{50}xC_{50}$ and $S_{100}xC_{100}$). The yield

373   difference for silage maize due to the combination of the average regional climate (C_{TUS}) with

374   soil input at 1 km resolution is zero towards the northern part, while it is positive from the

375   central to the southern part of Tuscany (Fig. 8, panel B: S_1xC_{Tus}). The pattern of yield

376   differences for silage maize in Tuscany based on simultaneous aggregation of soil and climate

377   input data is similar (Fig. 8, panel B: from $S_{10}xC_{10}$ to $S_{100}xC_{100}$, 1st row) to the pattern

378   observed when only soil is aggregated and combined with the average regional climate (Fig.

379   8, panel B: from $S_{10}xC_{Tus}$ to $S_{100}xC_{Tus}$, 2nd row). The yield differences are either positive or

380   zero for Tuscany when aggregation of climate input is combined with the dominant soil

381   (S_{TUS}) (Fig. 8, panel B, 3rd row).

382   **[Figure 8 Here]**

383   The aggregation effects on simulated silage maize yields are further analyzed as absolute

384   percentage yield difference (Eq. 1) from the yields simulated on the reference 1 km

385   resolution. The variability of absolute percentage yield difference for silage maize is

386   presented as box plots and its frequency distribution as violin plot for different aggregation

387   levels for NRW (Fig. 9A) and Tuscany (Fig. 9B). The absolute percentage yield differences

388   (%) for silage maize yield for the ensemble mean for combined soil and climate data

389   aggregation are in general higher for Tuscany than for NRW (Fig. 9). The mean absolute

390   percentage yield differences are ranging from 5 to 12 % in NRW and from 15 to 35 % in

391   Tuscany. Looking at the histograms, it becomes also clear, that the variability of the absolute

392   percentage yield differences in NRW can reach up to 40 % in some grid cells, and that it can

393   be even larger in Tuscany (>40%). On the other hand, lowest values of the absolute

394   percentage yield difference are between 0 to 5 % in NRW and 0 to 15 % in Tuscany.

395   **[Figure 9 Here]**

396   The aggregation effect at the regional scale quantified as the normalized or relative average

397   absolute yield deviation (rAAD) of silage maize yield in NRW is below 35 % for all crop

398   models regardless of the aggregation level of soil and climate input (Fig. 10, panel $S_y x C_z$)

399   whereas the rAAD increases with decreasing resolution. The rAAD is highest reaching 30 %

400   for the EPIC model followed by DayCent, when soil and climate input is aggregated to 100

401   km ($S_{100} x C_{100}$), and lowest for MONICA, which is always below 10%, while the ensemble

402   mean is about 10%. In contrast, when soil and climate input are aggregated, rAAD for the

403   maize simulations in Tuscany is much higher and reaches for DailyDayCent values of ~60 %.

404   Lowest values were found in Tuscany for CENTURY (<16%), indicating that the overall

405   spread of the model results is much larger compared to NRW. The larger spread but also the

406   higher values of rAAD for some models in Tuscany is also reflected in the rAAD of the

407   ensemble mean, which reaches 30% at the lowest input data resolution ($S_{100}xC_{100}$). However,

408   the effect of aggregating climate data, while keeping the dominant regional soil constant

409   (panels: $S_{NRW}xC_z$ and $S_{TUS}xC_z$), shows a completely different picture. In this case, the rAAD

410   seems to be relatively unaffected by the aggregation of climate inputs, and additionally, the

411   spread between models is even larger. When aggregating soil inputs and combining it with the

412   regional mean climate (S_yxC_{NRW} and S_yxC_{TUS}), the rAAD shows a similar pattern for

413   respective crop models as in the simultaneous aggregation of soil and climate inputs. Only

414   EPIC and CENTURY predicted decreased rAAD when decreasing soil resolution from 25 to

415   50 km for S_yxC_{TUS} in Tuscany.

416   **[Figure 10 Here]**

417   *3.2.2   Aggregation effect on winter wheat yield simulation in NRW and Tuscany*

418   As already shown for silage maize in NRW, the simultaneous aggregation of soil and climate

419   input to coarser resolutions of 50 and 100 km caused lower simulated wheat yields with

420   respect to the reference resolution (1 km). This is indicated by negative winter wheat yield

421   differences towards the North-Eastern part of NRW, while higher simulated yields with

422   positive yield differences are observed toward the South of NRW (Fig. 11, panel A: $S_{50}xC_{50}$

423   and $S_{100}xC_{100}$). A similar pattern is observed when aggregating soil input to 50 and 100 km

424   and combining it with the mean regional climate (Fig. 11, panel A: $S_{50}xC_{NRW}$ and $S_{100}xC_{NRW}$).

425   The aggregation of climate data at different resolutions with the dominant regional soil caused

426   higher simulated wheat yields than yield simulations for the reference resolution at 1km (Fig.

427   11, panel A: from $S_{NRW}xC_1$ to $S_{NRW}xC_{100}$). The mean yield differences for winter wheat in

428   NRW (Fig. 11, panel A) ranged from 0.01 to 1.0 t ha^{-1}. They increased when climate input

429   was aggregated from 1 to 100 km resolution and combined with the dominant regional soil

430   (Fig. 11, panel A: 3rd row). The mean absolute yield differences for winter wheat (AMD i.e.

431   numbers in each figures) are increasing with decreasing resolution of soil and climate input

432   data. The highest mean yield difference in NRW of 1 t ha^{-1} is observed for the combination of

433   dominant soil and 100 km climate aggregation ($S_{NRW}xC_{100}$). Again, the overall findings

434   indicate that the simultaneous aggregation of soil and climate input data has higher impact on

435   the mean yield difference than the aggregation of only soil or climate (Fig. 11 Panel A 1st

436   row).

437   **[Figure 11 Here]**

438   For Tuscany, the mean yield differences for wheat were at maximum 2 t ha^{-1}, mainly located

439   in the northern part, while for other parts of Tuscany slightly negative differences or no

440   difference occurred (Fig. 11, Panel B). In general, the mean yield difference of simulated

441   wheat yields for Tuscany increased with the combination of aggregated soil or climate input

442   to coarser resolutions (from 10 km to 100 km).

443   In comparison to NRW, the absolute percentage yield differences for winter wheat in Tuscany

444   has higher values, which range from 10 to 15 % when aggregating soil and climate input

445   simultaneously to coarser resolutions (Fig. 12). Additionally to the larger mean error, the

446   spread of the absolute percentage yield differences is also larger for Tuscany compared to

447   NRW. Aggregating soil input data, while keeping the climate input constant over the region

448   (C_{NRW} or C_{TUS}), indicates also an increasing trend of absolute percentage yield difference for

449   NRW. For Tuscany the absolute percentage yield differences increased with climate

450   resolution of 10 and 25 km and slightly decreased for resolutions of 50 and 100 km. Looking

451   at the histograms (Fig. 12) it becomes also visible that the aggregation of soil input data

452   combined with the dominant climate leads to large absolute percentage yield spreads between

453   the grid-cells. In both regions, the shape of the violin plots are similar, indicating that the

454   lower absolute percentage yield differences are found in a higher number of grid cells, while

455   only few pixels have very high absolute percentage yield differences (Fig. 12).

456   **[Figure 12 Here]**

457 The aggregation error for simulated wheat yields in NRW quantified at regional level as

458 normalized or relative average absolute yield deviation (rAAD) (Eq. 5) is below 30 % for

459 most of the crop models, while only two models HERMES and DailyDayCent show rAAD

460 values higher than 30 %, when climate input is aggregated and combined with the dominant

461 soil (Fig. 13NRW). For the combined aggregation of soil and climate input data (S_yxC_z), the

462 rAAD increases with decreasing resolution in both regions. However, maximum rAAD values

463 are observed in Tuscany reaching almost 50% with the EPIC model (Fig. 13 TUS). The

464 rAAD values for winter wheat are, in general, larger in Tuscany for the same aggregation

465 levels. The spread between the models is also larger in Tuscany compared to NRW, which

466 had been already observed for maize (Fig. 10). Thus, for simulation of winter wheat under

467 water limited conditions, the aggregation error at regional level shows an increasing trend

468 when soil and climate input data are simultaneously aggregated to the coarser resolutions

469 regardless of the region (Fig. 13: panels S_yxC_z). The increase of rAAD is less pronounced in

470 winter wheat simulations, when only climate or soil input is aggregated except for climate

471 input aggregation combined with the dominant soil in Tuscany (Fig 13 TUS).

472   **[Figure 13 Here]**

473 # 4   Discussion

474 ## 4.1   Input data aggregation and main effect in simulated yield

475 Crop model simulations depend highly on the availability and reliability of input data for soil

476 parameter and climate variables. As Ewert et al. (2015, 2011) already stated, the spatial

477 aggregation of input data from local to regional scale reduces the variability of these data.

478 Furthermore, the deformation of data for different climatic variables when aggregated from

479 higher resolution of 1 km to coarser resolution of 10, 25, 50, and 100 km is evaluated in

480 Hoffmann et al. (2017), indicating that the spatial variability of climatic variables decreases

481   due to data aggregation (1 to 100 km) with similar mean values (Hoffmann et al., 2015). For

482   example, in the mountainous Northwestern part of Tuscany, the low values for daily

483   minimum temperature detectable at 1 km resolution are averaged out at coarser resolutions of

484   100 km (Fig. 4). The same applies to the higher temperatures at 1 km resolution at the

485   southern edge of the region (Fig. 4). This means that the aggregation of data in heterogeneous

486   areas has stronger impacts on the extreme than on the mean values. The same feature of a loss

487   of extreme values has been also reported for temporal aggregation of climatic data by

488   Weihermuller et al. (2011).

489   As shown in the results there are common trends in the simulated yields as a function of input

490   data aggregation in NRW and Tuscany but also differences are detectable between the two

491   study regions:

492   1. Combined aggregation of soil and climate lead to an increase of the error in simulated

493   yields with decreasing resolution for both winter and spring crop.

494   2. Aggregation of soil data inputs, while keeping the mean regional climate, shows, in

495   NRW, comparable effects on the aggregation error in simulated yields as a combined

496   aggregation of soil and climate for both winter and spring crop. However, in Tuscany

497   the aggregation error due to soil data aggregation is generally higher regardless of the

498   resolution.

499   3. Aggregation of climate data inputs to coarser resolutions, while keeping the dominant

500   regional soils, shows variable effects on the error in simulated yields and changes only

501   little with increasing resolution for both winter and spring crop (wheat and maize) for

502   both study regions.

503   4. The Mediterranean region (Tuscany) shows larger spread between the models and

504   larger aggregation errors.

505   Point 1 and 2 has been already reported for NRW by Hoffmann et al. (2017) but due to the

506   limitation of the study to one region no generalization could be made. By analyzing the

507   aggregation effect as average absolute percentage difference between grid cell yields at the

508   coarse resolutions (20, 25, 50, 100 km) compared to the finest resolution (1 km) for two

509   contrasting regions (NRW and Tuscany) it becomes evident, that soil aggregation has a

510   stronger impact in Tuscany compared to NRW for both crops. When analyzing the absolute

511   bias of average simulated yields, this is only evident for silage maize. . In contrast,

512   disaggregation of soil data from coarser resolution (2.8^0x2.8^0) to finer resolution (1^0x1^0) did

513   not improve the regional yield simulation of grain maize in the central US Great Plains

514   (Easterling et al., 1998). Increasing resolution of climate data using the same soil as model

515   input, did hardly increase the aggregation error, although the assumption of one dominant soil

516   over the whole region had strong effects on the mean absolute yield difference (AMD, Figs. 8

517   and 11) and on the average absolute percentage yield difference (Figs. 9 and 12) except for

518   winter wheat in Tuscany. The impact of climatic data aggregation on simulated crop yield has

519   been studied by Zhao et al. (2015b) who related the spatial variability of climatic data to

520   topographic features (mainly elevation) in the landscape. Hereby, they found that flat and

521   more homogeneous areas can be aggregated to coarser resolution without increasing the

522   aggregation error, while more heterogeneous landscapes react differently with much larger

523   aggregation errors. The aggregation effect of climate data for winter wheat for a Scandinavian

524   region in Finland was also evaluated by Angulo et al. (2013), who stated that simulated yield

525   distributions are similar and independent of the resolution of the climate input data. As both

526   regions analyzed in our study are rather heterogeneous in terms of elevation and climate, an

527   effect of the aggregation of climate data on the simulated yields could be expected, but the

528   effect was relatively small (Figs. 8, 9, 11 and 12), which could be due to the strong influence

529   of the choice of the dominant regional soil (S_{TUS} and S_{NRW}).

530   Depending on the extent of heterogeneity in topographic and climatic features, there is a

531   threshold of the data resolution where the data aggregation effect on model simulation error

532   is minimized. This has been investigated in Zhao et al. (2015b), defining the requirement of

533   data at high resolution in topographically heterogeneous regions compared to plain areas. For

534   the aggregation of soils, the soil properties at the field level are aggregated to the regional

535   level. The aggregation of soil properties from fine to coarser resolution is classically done by

536   selecting the dominant soil type with a corresponding reference soil profile rather than

537   averaging soil properties. The reasons not to use spatial averaging is quite obvious, because

538   averaging e.g. soil texture is associated with considerable problems. For example, a grid cell

539   containing an entirely sandy soil for half of its area with the other half a clayey textured soil

540   throughout the rooting zone would provide a sandy clay on average, which adequately reflects

541   neither the physical properties of sandy soil material nor those of clayey soil material. On the

542   other hand, aggregation by dominant soil type will lead to a loss of information in the

543   simulated outputs because non-dominant but functionally very differently behaving soils will

544   not be taken into account during the model runs at coarser resolutions (10-100 km)

545   (Coucheney et al., 2018). In consequence, model responses (in our case yield) from non-

546   dominant areas of the grid cell will not be reproduced at large scale. The effect of different

547   aggregation or scaling approaches on soil hydraulic properties has been studied by Montzka et

548   al. (2017) but the propagation of the different outputs through non-linear models such as crop

549   growth models has not been analyzed.

550   The application of soil data aggregation to coarser resolution has considerable impact on

551   simulated crop yields and induces biased results at the regional scale at coarser resolutions.

552   Therefore, in the next chapter, the quantification of the aggregation error in simulated crop

553   yields for maize (spring crop) and winter wheat (winter crop) will be discussed.

554   **4.2   Aggregation error on crop yield simulations**

555   *4.2.1   Winter wheat*

556   The aggregation effect of climate data was evaluated for winter wheat for a Scandinavian

557   region in Finland (Angulo et al., 2013) and the aggregation effect of soil data on simulated

558   yields of winter wheat was evaluated for a region with a temperate climate in Germany

559   (Angulo et al., 2014). Angulo et al. (2014) used the frequency distribution of crop yields as a

560   characteristic fingerprint to compare the effect of input data aggregation between crop models

561   and input data resolutions. They found that the fingerprints were similar for the different

562   resolutions of climate input data, while they varied across the different models applied. In line

563   with these results, the distribution of simulated winter wheat yield in NRW did not differ

564   much between different resolutions of climate input. However, in Tuscany, the range of the

565   frequency distribution and the average absolute percentage yield difference increased with

566   decreasing resolution of climate input data (Fig. 12B, climate aggregation panel). Aggregating

567   soil types at 1 km^2 resolution to the dominant soil in a coarser grid cell without aggregating

568   the climate variables, tends to cause a positive bias in wheat yields in both regions (Figure

569   11A and B, row 2). This indicates, that in both regions the more productive soils for winter

570   wheat were dominant in most of the grid cells in the different resolutions. However, there

571   were two instances where the positive wheat yield bias decreased when changing from the 10

572   km resolution (S_{10} x C_z) to the 25 km resolution (S_{25} x C_z) in both regions. Additionally, the

573   combination of dominant soil at regional level with aggregated climate for both regions

574   showed positive yield bias for winter wheat simulation (Fig. 11, row 3). This indicates the

575   highly productive characteristics of aggregated soil at regional level leading to positive

576   simulated yield bias. Here it has to be noted that, if the aggregated soil at regional level would

577   have been a less productive soils, a negative yield bias would have been observed in the

578   simulations.

579   In NRW, the range and the mean of the absolute percentage yield difference increased when

580   both soil and climate input data were aggregated, while in Tuscany only the mean of absolute

581   percentage yield difference increased but not the range. For winter wheat, the aggregation

582   effect on the ensemble yield due to aggregated climate data (1 to 100 km), quantified as

583   relative average absolute deviation (rAAD), was maximum up to 10 % (Zhao et al., 2015a)

584   with mean of 3-5 % for NRW, while we have found maximum rAAD of 38% and 50% for

585   NRW and Tuscany respectively and around 15% for the ensemble mean in both regions (Fig.

586   13). These values did not change when combinations of aggregated soil and climate data were

587   used in the ensemble simulations. Thus, for winter wheat, the average error of climate data

588   aggregation combined with regional soil type over the model ensemble is between 10 and 15

589   % in both regions. However, the uncertainties in the aggregation error for winter wheat yields

590   are higher in Tuscany as shown in the wider range of the mean absolute yield difference and

591   the relative rAAD in Tuscany (Fig. 12 and 13). Thus, the uncertainty in the aggregation effect

592   for the winter crop in the temperate regions due to input data aggregation (irrespective of

593   climate or soil data) is lower compared to the Mediterranean region probably due to the, on

594   average, positive climatic water balance and the higher water holding capacity (Hoffmann et

595   al., 2015).

596   With respect to the differences in aggregation error for simulated wheat yields between the

597   single models, there is no evident consistency in the obtained results, except that the EPIC

598   model could be classified as more sensitive to soil and climate data aggregation, having both

599   in Tuscany and NRW relative rAADs above the ensemble mean, whereas the STICS model

600   belongs to the less sensitive models with relative rAADs close to the ensemble mean. This

601   may be due to differences in reference evapotranspiration (Penman-Monteith against

602   Priestley- Taylor) and in approaches to calculate light absorption (one leaf versus multi-layer

603   approach) (Brisson et al., 1998).

604   *4.2.3   Silage maize*

605   The mere aggregation of the soil types according to the dominant soil in the coarser grid cell,

606   caused a positive bias in silage maize yields in both regions (Figure 8A and B, row 2) as

607   previously observed for wheat yields. In both regions, the more productive soils seem to be

608   dominant in most of the grid cells, although the positive bias strongly decreased in Tuscany

609   from a mean yield difference of 1.24 t ha^{-1} to 0.43 t ha^{-1} when changing from the 1 km

610   resolution (S$_1$ x C$_{TUS}$) to the 25 km resolution (S$_{25}$ x C$_{TUS}$).

611   The combined aggregation of soil and climate input data caused an increase in median and

612   average absolute percentage yield difference of silage maize with decreasing resolution (Fig.

613   9). This has been already shown by Hoffman et al. (2016) for NRW. However, in contrast, to

614   the winter crop (wheat), the range and average absolute percentage yield differences due to

615   climate and soil input data aggregation for silage maize were much higher in Tuscany

616   compared to NRW. This observation was also made when only climate input data were

617   aggregated. Thus, irrespective of the kind of input data aggregated, simulated maize yields in

618   the Mediterranean region showed higher absolute percentage yield differences compared to

619   the temperate region already at resolutions of 10 km. At a resolution of 100 km, the absolute

620   percentage yield differences were higher by a factor of up to 3 compared to the temperate

621   region when both soil and climate data were aggregated (Fig. 9). This has been corroborated

622   by the results published by Folberth et al. (2014) for the US and could be explained by the

623   difference in climate conditions between the temperate and Mediterranean site, which is

624   higher during the vegetation period of the spring crops compared to the winter crop (Table 3).

625   The average precipitation in Tuscany and NRW during the growing period of silage maize is

626   around 350 mm in both regions, whereas the mean temperature is much lower in the

627   temperate region (15.7 and 21.7 °C in NRW and Tuscany, respectively). Thus, warmer and

628   drier conditions during the growing period tend to translate into higher aggregation errors in

629   regional crop simulations. These results are confirmed by the higher relative rAAD of

630   ensemble yields of maize compared to winter wheat in both regions (Fig. 10 and 13). With

631   respect to maize yields, relative rAAD in Tuscany increases stronger compared to NRW when

632   the resolution of input data is decreasing (Fig. 10). In both regions, the increase in relative

633   rAAD from fine to coarse resolution is strongest when aggregation of climate data is

634   combined with aggregation of soil input data and can reach an average relative rAAD of the

635   ensemble mean of 25%. Extreme model-dependent relative rAAD for maize yields can reach

636   58% in Tuscany compared 38% in NRW. In the case of the spring crop (maize), the

637   aggregation error of the ensemble mean reaches already 20% when a resolution of 10 km for

638   the soil or climate data is used, whereas in NRW such high aggregation errors are never

639   reached with simulated maize yields regardless of the spatial resolution of soil and climate

640   data. These results suggest that reliable regional simulation of spring crop yield in

641   Mediterranean climate conditions requires high spatial resolution of both soil and climate

642   data.

643   Looking at the differences between the individual models in the aggregation error for

644   simulated maize yields, DailyDayCent seems to be most sensitive to soil aggregation or the

645   combined aggregation of soil and climate input data both in NRW (together with EPIC) and

646   in Tuscany (Fig. 10). In NRW, this is consistent with the findings for maize yield simulations

647   (Fig. 10). Thus, there is no single explanation, which can explain the differences in sensitivity

648   to input data aggregation among the individual models. This may require further analysis of

649   relationships between aggregation errors and modeling approaches of certain processes.

650   **4.3   Hotspots of aggregation errors**

651   Looking at the spatial variability of the average yield differences (Fig. 8 and 11), we were

652   able to identify several hotspots where the simulated yields of both crops were very sensitive

653   to data aggregation by producing large yield differences (-6 to 6 t ha^{-1} for silage maize, -2 to 2

654   t ha^{-1} for winter wheat) (Fig. 8 and 11). In NRW, the spatial patterns of yield differences due

655   to the simultaneous aggregation of soil and climate input data (Fig. 8 and 11 Panel A, first

656   row) and due to aggregation of soil input data only (Fig. 8 and 11 Panel A, second row) are

657   similar for both crops. The largest wheat and maize yield differences in NRW due to

658   aggregation of soil are found in the Northeast and in two smaller areas in the Northwest and

659   Central-South with average yield difference of more than 3 t ha^{-1} in the case of maize. This

660   indicates that aggregation of soil data is the main driver to induce aggregation errors in NRW.

661   In Tuscany, a similar trend is observed with stronger spatial differentiation of yield

662   differences due to aggregation of soil input data or the combination of soil and climate input

663   data (Fig. 8 and 11 Panel B, first and second row). However, in Tuscany, the hot spots with

664   highest yield differences for maize depend on the resolution, with underestimations being

665   concentrated in the Center and Northwest of Tuscany for resolutions of 10 and 25 km and

666   with underestimations in the Central and Southern part of Tuscany and overestimations in the

667   North for resolutions of 50 and 100 km. In the case of winter wheat, the location of hot spots

668   is similar, but overestimations with strongly positive yield differences are more prominent in

669   the Northern part of Tuscany toward the Northern mountain ranges. In the Northern mountain

670   region with sharp spatial gradients of temperature, the aggregation of climate input data by

671   the average method eliminates the extreme values which exist at 1 km resolution (Hoffmann

672   et al., 2015) and results in on average moderate temperature for coarser resolutions. Thus,

673   aggregation in the mountain regions produces more favourable environmental conditions in

674   the input data set of the coarser resolutions, leading to higher simulated crop yields. While in

675   the central and Southern part of Tuscany, aggregation of climate data causes negative yield

676   differences because small hilly areas with higher precipitation are averaged out, leading to on

677   average lower precipitation at coarser resolutions. An a priori identification of such sensitive

678   areas to spatial aggregation errors in terms of soil and climate characteristics would therefore

679   help defining the appropriate grid resolution over the region being investigated.

680   **4.4**   **Influence of the range in altitude on the magnitude of aggregation errors**

681   As the effects of climate input data aggregation on aggregation errors in crop yields is

682   obviously stronger in Tuscany, it could be argued that this is due the topographically stronger

683   climatic gradient within Tuscany. The range in altitude is larger in Tuscany (0-1875 m)

684   compared to NRW (0-845). However, if we eliminate the grid cells in Tuscany, which have

685   an elevation above 845 m, to have a comparable range of altitude in both regions, the

686   aggregation effects of soil and climate input on crop yields are still significantly different

687   between the two regions (Fig. S1, 10 and 13). For simulated wheat yields, the rAADs in the

688   coarser resolutions (50 and 100 km) even increase when eliminating grids with altitudes

689   greater than 845 m. This supports our findings that the higher aggregation effects in Tuscany

690   compared to NRW are mainly due to the differences in climatic conditions.

691   # 5   Conclusion

692   The aggregation effects of soil and climate data on crop yield simulations in the

693   Mediterranean region are higher than in the temperate region in particular for the spring crop

694   (silage maize). The magnitude of the aggregation effect in Tuscany for silage maize expressed

695   as the percentage absolute yield difference is on average 30% compared to an average of 10

696   % for winter wheat. Because of the higher aggregation effect on crop yield simulation in the

697   Mediterranean region, it is important in these regions to use input data at a finer resolution for

698   reliable estimation of regional crop yield. Moreover, in each region, there are hot spots with

699   extremely high positive or negative yield differences due to input data aggregation. In these

700   hot spots, a finer resolution of climate and in particular soil information is important to reduce

701   errors in crop yield simulations. For generalization of these outcomes, further investigations

702   in other sub-humid or semi-arid regions will be necessary. This would further help in

703   understanding and conceptualizing how various climatic conditions and soil variability

704   interactions make the data aggregation effect vary and to identify which conditions are critical

705 to take into account when deciding the adequate grid resolution for reliable simulation of
706 regional crop yield.

Acknowledgements

References

Allen, R.G., Pereira, L.S., Raes, D., Smith, M., 1998. FAO Irrigation and Drainage Paper Crop by. Irrig. Drain. 300, 300. https://doi.org/10.1016/j.eja.2010.12.001

Angulo, C., Gaiser, T., Rötter, R.P., Børgesen, C.D., Hlavinka, P., Trnka, M., Ewert, F., 2014. "Fingerprints" of four crop models as affected by soil input data aggregation. Eur. J. Agron. 61, 35–48. https://doi.org/10.1016/j.eja.2014.07.005

Angulo, C., Rötter, R., Trnka, M., Pirttioja, N., Gaiser, T., Hlavinka, P., Ewert, F., 2013. Characteristic "fingerprints" of crop model responses to weather input data at different spatial resolutions. Eur. J. Agron. 49, 104–114. https://doi.org/10.1016/j.eja.2013.04.003

Bergez, J.-E., Chabrier, P., Gary, C., Jeuffroy, M.H., Makowski, D., Quesnel, G., Ramat, E., Raynal, H., Rousse, N., Wallach, D., Debaeke, P., Durand, P., Duru, M., Dury, J., Faverdin, P., Gascuel-Odoux, C., Garcia, F., 2013. An open platform to build, evaluate and simulate integrated models of farming and agro-ecosystems. Environ. Model. Softw. 39, 39–49. https://doi.org/10.1016/J.ENVSOFT.2012.03.011

Brisson, N., Launay, M., Mary, B., Beaudoin, N., 2009. Conceptual basis, formalisations and parameterisation of the STICS crop model.

Brisson, N., Mary, B., Ripoche, D., Jeuffroy, M.H., Ruget, F., Nicoullaud, B., Gate, P., Devienne-Barret, F., Antonioletti, R., Durr, C., Richard, G., Beaudoin, N., Recous, S., Tayot, X., Plenet, D., Cellier, P., Machet, J.-M., Meynard, J.M., Delécolle, R., 1998. STICS: a generic model for the simulation of crops and their water and nitrogen balances. I. Theory and parameterization applied to wheat and corn. Agronomie 18, 311–346. https://doi.org/10.1051/agro:19980501

Conrad, Y., Fohrer, N., 2009. Modelling of nitrogen leaching under a complex winter wheat and red clover crop rotation in a drained agricultural field. Phys. Chem. Earth 34, 530–

753   540. https://doi.org/10.1016/j.pce.2008.08.003

754   Coucheney, E., Eckersten, H., Hoffmann, H., Jansson, P.E., Gaiser, T., Ewert, F., Lewan, E.,

755   2018. Key functional soil types explain data aggregation effects on simulated yield, soil

756   carbon, drainage and nitrogen leaching at a regional scale. Geoderma 318, 167–181.

757   https://doi.org/10.1016/j.geoderma.2017.11.025

758   Del Grosso, S., Parton, W., Mosier, A., Hartman, M., Brenner, J., Ojima, D., Schimel, D.,

759   2001. Simulated Interaction of Carbon Dynamics and Nitrogen Trace Gas Fluxes Using

760   the DAYCENT Model, Modeling Carbon and Nitrogen Dynamics for Soil Management.

761   CRC Press. https://doi.org/10.1201/9781420032635.ch8

762   Del Grosso, S.J., Parton, W.J., Mosier, A.R., Walsh, M.K., Ojima, D.S., Thornton, P.E., 2006.

763   DAYCENT National-Scale Simulations of Nitrous Oxide Emissions from Cropped Soils

764   in the United States. J. Environ. Qual. 35, 1451. https://doi.org/10.2134/jeq2005.0160

765   Donatelli, M., Srivastava, A.K., Duveiller, G., Niemeyer, S., Fumagalli, D., 2015. Climate

766   change impact and potential adaptation strategies under alternate realizations of climate

767   scenarios for three major crops in Europe. Environ. Res. Lett. 10.

768   https://doi.org/10.1088/1748-9326/10/7/075005

769   Easterlinga, W.E., Weiss, A., Hays, C.J., Mearns, L.O., 1998. Spatial scales of climate

770   information for simulating wheat and maize productivity: the case of the US Great

771   Plains. Agric. For. Meteorol. 90, 51–63. https://doi.org/10.1016/S0168-1923(97)00091-9

772   Ewert, F., Bussel, L.G.J. Van, Zhao, G., Hoffmann, H., 2015. Uncertainties in Scaling-Up

773   Crop Models for Large-Area Climate Change [WWW Document].

774   Ewert, F., Rötter, R.P., Bindi, M., Webber, H., Trnka, M., Kersebaum, K.C., Olesen, J.E., van

775   Ittersum, M.K., Janssen, S., Rivington, M., Semenov, M.A., Wallach, D., Porter, J.R.,

776   Stewart, D., Verhagen, J., Gaiser, T., Palosuo, T., Tao, F., Nendel, C., Roggero, P.P.,

777   Bartosˇová, L., Asseng, S., 2015. Crop modelling for integrated assessment of risk to

778   food production from climate change. Environ. Model. Softw. 72, 287–303.

779   https://doi.org/10.1016/j.envsoft.2014.12.003

780   Ewert, F., van Ittersum, M.K., Heckelei, T., Therond, O., Bezlepkina, I., Andersen, E., 2011.

781   Scale changes and model linking methods for integrated assessment of agri-

782   environmental systems. Agric. Ecosyst. Environ. 142, 6–17.

783   https://doi.org/10.1016/j.agee.2011.05.016

784   Gaiser, T., Perkons, U., Küpper, P.M., Kautz, T., Uteau-Puschmann, D., Ewert, F., Enders,

785   A., Krauss, G., 2013. Modeling biopore effects on root growth and biomass production

786   on soils with pronounced sub-soil clay accumulation. Ecol. Modell. 256, 6–15.

787   https://doi.org/10.1016/J.ECOLMODEL.2013.02.016

788   Klosterhalfen, A., M. Herbst, L. Weihermüller, A. Graf, M. Schmidt, A. Stadler, K.

789   Schneider, J.-A. Subke, J.A. Huisman, and H. Vereecken 2017. Multi-site calibration and

790   validation of a net ecosystem carbon exchange model for croplands. Ecol. Modell. 363:

791   137–156.

792   Hansen, S., Abrahamsen, P., Petersen, C.T., Styczen, M., 2012. DAISY: MODEL USE,

793   CALIBRATION, AND VALIDATION 55, 1315–1333.

794   Herbst, M., Hellebrand, H.J., Bauer, J., Huisman, J.A., Šimůnek, J., Weihermüller, L., Graf,

795   A., Vanderborght, J., Vereecken, H., 2008. Multiyear heterotrophic soil respiration:

796   Evaluation of a coupled CO_2 transport and carbon turnover model. Ecol. Modell. 214,

797   271–283. https://doi.org/10.1016/J.ECOLMODEL.2008.02.007

798   Hintze, L., Nelson, R.D., 1998. Violin Plots: A Box Plot-Density Trace Synergis. Am. Stat.

799   52, 181–184.

800   Hoffmann, H., Baranowski, P., Krzyszczak, J., Zubik, M., Sławiński, C., Gaiser, T., Ewert, F.,

801   2017. Temporal properties of spatially aggregated meteorological time series. Agric. For.

802   Meteorol. 234–235, 247–257. https://doi.org/10.1016/j.agrformet.2016.12.012

803 Hoffmann, H., Zhao, G., Asseng, S., Bindi, M., Biernath, C., Constantin, J., Coucheney, E.,

804   Dechow, R., Doro, L., Eckersten, H., Gaiser, T., Grosz, B., Heinlein, F., Kassie, B.T.,

805   Kersebaum, K.C., Klein, C., Kuhnert, M., Lewan, E., Moriondo, M., Nendel, C.,

806   Priesack, E., Raynal, H., Roggero, P.P., Rötter, R.P., Siebert, S., Specka, X., Tao, F.,

807   Teixeira, E., Trombi, G., Wallach, D., Weihermüller, L., Yeluripati, J., Ewert, F., 2016.

808   Impact of spatial soil and climate input data aggregation on regional Yield Simulations.

809   PLoS One 11, 1–23. https://doi.org/10.1371/journal.pone.0151782

810 Hoffmann, H., Zhao, G., Van Bussel, L.G.J., Enders, A., Specka, X., Sosa, C., Yeluripati, J.,

811   Tao, F., Constantin, J., Raynal, H., Teixeira, E., Grosz, B., Doro, L., Zhao, Z., Wang, E.,

812   Nendel, C., Kersebaum, K.C., Haas, E., Kiese, R., Klatt, S., Eckersten, H., Vanuytrecht,

813   E., Kuhnert, M., Lewan, E., Rötter, R., Roggero, P.P., Wallach, D., Cammarano, D.,

814   Asseng, S., Krauss, G., Siebert, S., Gaiser, T., Ewert, F., 2015. Variability of effects of

815   spatial climate data aggregation on regional yield simulation by crop models. Clim. Res.

816   65, 53–69. https://doi.org/10.3354/cr01326

817 Kersebaum, K.C., 2007. Modelling nitrogen dynamics in soil-crop systems with HERMES.

818   Nutr. Cycl. Agroecosystems 77, 39–52. https://doi.org/10.1007/s10705-006-9044-8

819 Liang, H., Hu, K., Batchelor, W.D., Qi, Z., Li, B., 2016. An integrated soil-crop system model

820   for water and nitrogen management in North China. Sci. Rep. 6, 1–20.

821   https://doi.org/10.1038/srep25755

822 Montzka, C., Herbst, M., Weihermüller, L., Verhoef, A., Vereecken, H., 2017. A global data

823   set of soil hydraulic properties and sub-grid variability of soil water retention and

824   hydraulic conductivity curves. Earth Syst. Sci. Data Discuss. 1–25.

825   https://doi.org/10.5194/essd-2017-13

826   Nendel, C., Berg, M., Kersebaum, K.C., Mirschel, W., Specka, X., Wegehenkel, M., Wenkel,

827   K.O., Wieland, R., 2011. The MONICA model: Testing predictability for crop growth,

828   soil moisture and nitrogen dynamics. Ecol. Modell. 222, 1614–1625.

829   https://doi.org/10.1016/j.ecolmodel.2011.02.018

830   Rosenzweig, C., Elliott, J., Deryng, D., Ruane, A.C., Müller, C., Arneth, A., Boote, K.J.,

831   Folberth, C., Glotter, M., Khabarov, N., Neumann, K., Piontek, F., Pugh, T.A.M.,

832   Schmid, E., Stehfest, E., Yang, H., Jones, J.W., 2014. Assessing agricultural risks of

833   climate change in the 21st century in a global gridded crop model intercomparison. Proc.

834   Natl. Acad. Sci. 111, 3268–3273. https://doi.org/10.1073/pnas.1222463110

835   Rosenzweig, C., Iglesias, A., 1998. The use of crop models for international climate change

836   impact assessment 267–292. https://doi.org/10.1007/978-94-017-3624-4_13

837   Rosenzweig, C., Parry, M.L., 1994. Potential impact of climate change on world food supply.

838   Nature 367, 133–138. https://doi.org/10.1038/367133a0

839   Shibu, M.E., Leffelaar, P.A., van Keulen, H., Aggarwal, P.K., 2010. LINTUL3, a simulation

840   model for nitrogen-limited situations: Application to rice. Eur. J. Agron. 32, 255–271.

841   https://doi.org/10.1016/J.EJA.2010.01.003

842   Singh, A.K., Goyal, V., Mishra, A.K., Parihar, S.S., 2013. Validation of CropSyst simulation

843   model for direct seeded rice – wheat cropping system. Curr. Sci. 104, 1324–1331.

844   Specka, X., Nendel, C., Wieland, R., 2015. Analysing the parameter sensitivity of the agro-

845   ecosystem model MONICA for different crops. Eur. J. Agron. 71, 73–87.

846   https://doi.org/10.1016/J.EJA.2015.08.004

847   Thornton, P.E., Hasenauer, H., White, M.A., 2000. Simultaneous estimation of daily solar

848   radiation and humidity from observed temperature and precipitation: An application over

849   complex terrain in Austria. Agric. For. Meteorol. 104, 255–271.

850 https://doi.org/10.1016/S0168-1923(00)00170-2

851 Weihermuller, L., Huisman, J.A., Graf, A., Herbst, M., Vereecken, H., 2011. Errors in

852 Modeling Carbon Turnover Induced by Temporal Temperature Aggregation. Vadose Zo.

853 J. 10, 195–205. https://doi.org/10.2136/vzj2009.0157

854 Zhao, G., Hoffmann, H., Van Bussel, L.G.J., Enders, A., Specka, X., Sosa, C., Yeluripati, J.,

855 Tao, F., Constantin, J., Raynal, H., Teixeira, E., Grosz, B., Doro, L., Zhao, Z., Nendel,

856 C., Kiese, R., Eckersten, H., Haas, E., Vanuytrecht, E., Wang, E., Kuhnert, M., Trombi,

857 G., Moriondo, M., Bindi, M., Lewan, E., Bach, M., Kersebaum, K.C., Rötter, R.,

858 Roggero, P.P., Wallach, D., Cammarano, D., Asseng, S., Krauss, G., Siebert, S., Gaiser,

859 T., Ewert, F., 2015a. Effect of weather data aggregation on regional crop simulation for

860 different crops, production conditions, and response variables. Clim. Res. 65, 141–157.

861 https://doi.org/10.3354/cr01301

862 Zhao, G., Siebert, S., Enders, A., Rezaei, E.E., Yan, C., Ewert, F., 2015b. Demand for multi-

863 scale weather data for regional crop modeling. Agric. For. Meteorol. 200, 156–171.

864 https://doi.org/10.1016/j.agrformet.2014.09.026

865

866

List of table captions

867

868 **Table 1:** Main climatic variables for the time period 1995 to 2011 for NRW and TUS. Mean
869 is the arithmetic mean, STD is the standard deviation, and 25, 50, 75 % are the
870 respective percentiles (Mean annual values and temporal variability)

871 **Table 2:** Total soil depth and soil properties of the top soil layer in NRW and Tuscany at 1x1
872 km resolution

873 **Table 3:** Summary of climatic condition during the growing period of silage maize and winter
874 wheat for NRW and Tuscany (1995-2011)

875 **Table 4:** List of crop models used in the model ensemble

876 **Table 5:** Crop management of winter wheat and silage maize in Tuscany

877 **Table 6:** Crop management of winter wheat and silage maize in NRW

878 **Table 7:** The abbreviation for input data combination of soil and climate data at different
879 resolutions.

880

881 **Table 1. Main climatic variables for the time period 1995 to 2011 for NRW and TUS. Mean is**

882 **the arithmetic mean, STD is the standard deviation, and 25, 50, 75 % are the respective**

883 **percentiles (Mean annual values and temporal variability)**

Climate variable[*]	Summary statistics for climate variables						
NRW	Mean	STD	Minimum	25 %	50 %	75 %	Maximum
TempMin (^{o}C)	5.6	0.7	3.9	5.4	5.6	6.0	6.7
TempMean (^{o}C)	9.6	0.7	7.6	9.4	9.6	10.1	10.3
TempMax (^{o}C)	13.7	0.8	11.5	13.5	13.9	14.2	14.7
Radiation(MJ m^{-2} d^{-1})	10.4	0.4	9.6	10.1	10.4	10.6	11.5
Windspeed (m s^{-1})	2.6	0.1	2.4	2.5	2.6	2.7	2.8
Precipitation (mm y^{-1})	821.1	117.3	659.1	752.3	801.3	861.7	1022.5
ET$_0$	986.6	56.3	875.7	947.7	986.4	1019.2	1100.2
cwb	165	147	-122	101	197	231	425
Tuscany	Mean	STD	Minimum	25 %	50 %	75 %	Maximum
TempMin (^{o}C)	8.8	0.4	8.0	8.7	8.8	9.1	9.3
TempMean (^{o}C)	16.1	0.5	15.1	15.8	16.2	16.5	16.8
TempMax (^{o}C)	18.6	0.6	17.4	18.1	18.7	19.0	19.4
Radiation(MJ m^{-2} d^{-1})	14.2	0.5	12.8	14.0	14.3	14.5	15.1
Wind speed (m s^{-1})	2.0	0.1	1.7	1.9	2.0	2.1	2.3
Precipitation (mm y^{-1})	949.4	192.5	667.8	809.1	967.8	1035.6	1424.8
ET$_0$ (mm y^{-1})	1495.8	64.3	1335.3	1460.8	1524.3	1531.8	1626.1
cwb (mm y^{-1})	546	244	-89	441	527	733	858

884 *TempMin: Minimum Temperature, TempMean: Mean Temperature, TempMax: Maximum

885 Temperature, ET$_0$: Reference Evapotranspiration (calculated by using ET$_0$ equation in FAO 56) , cwb:

886 Climate water balance (ET$_0$ − Precipitation) and others are as indicated

887

888

889 **Table: 2. Total soil depth and soil properties of the top soil layer in NRW and Tuscany at 1x1**

890 **km resolution**

NRW	Number of pixels	mean	std	min	25%	50%	75%	max
Depth [m]		0.29	0.03	0.10	0.30	0.30	0.30	0.30
Sand [%]		37.66	29.76	5.00	15.00	18.00	64.00	92.00
BD [g cm-3]		1.40	0.02	0.56	1.40	1.40	1.40	1.40
Wilting point [m3 m-3]	34168	0.14	0.06	0.04	0.09	0.16	0.18	0.29
Field capacity [m3 m-3]		0.26	0.08	0.12	0.20	0.29	0.33	0.39

TUS	Number of pixels	mean	std	min	25%	50%	75%	max
Depth [m]		0.49	0.04	0.18	0.50	0.50	0.50	0.50
Sand [%]		33.27	16.51	2.00	22.25	30.75	46.80	89.75
BD [g cm-3]		1.38	0.12	0.73	1.34	1.40	1.46	1.71
Wilting point [m3 m-3]	22933	0.10	0.02	0.05	0.08	0.10	0.12	0.20
Field capacity [m3 m-3]		0.26	0.04	0.06	0.24	0.27	0.28	0.38

891

892 **Table 3: Summary of climatic condition during the growing period of silage maize and winter**

893 **wheat for NRW and Tuscany (1995-2011)**

Climate variable	Summary statistics for climate variables during maize growing season							
NRW		Mean	STD	Minimum	25 %	50 %	75 %	Maximum
TempMin (ºC)		10.6	0.6	9.5	10.3	10.6	11.0	11.6
TempMean (ºC)		15.7	0.6	14.2	15.3	15.7	15.9	17.2
TempMax (ºC)		20.9	0.8	19.2	20.5	20.8	21.2	22.9
Radiation(MJ m^{-2} d^{-1})		16.8	0.7	15.4	16.3	16.8	17.2	18.1
Windspeed (m s^{-1})		2.3	0.1	2.1	2.2	2.3	2.4	2.6
Precipitation (mm y^{-1})		357.6	56.3	276.2	316.4	356.3	378.2	496.2
ET$_0$		686.0	40.2	616.3	670.8	685.7	708.0	770.0
cwb		328.4	85.8	174.7	286.2	324.3	385.4	469.8
Tuscany		Mean	STD	Minimum	25 %	50 %	75 %	Maximum
TempMin (ºC)		13.1	0.6	12.1	12.6	13.1	13.4	14.4
TempMean (ºC)		21.7	0.8	20.4	21.1	21.5	22.1	23.6
TempMax (ºC)		24.6	0.9	23.2	23.8	24.5	24.9	26.6

Climate variable	Mean	STD	Minimum	25 %	50 %	75 %	Maximum
Radiation (MJ m^{-2} d^{-1})	21.2	0.6	19.5	20.8	21.3	21.6	22.2
Windspeed (m s^{-1})	1.9	0.1	1.7	1.8	1.9	2.0	2.1
Precipitation (mm y^{-1})	354.3	88.7	219.4	315.3	323.9	397.1	531.7
ET$_0$ (mm y^{-1})	1130.3	47.2	1033.7	1098.6	1141.3	1156.6	1237.8
cwb (mm y^{-1})	776.0	130.0	502.0	721.7	785.5	838.3	1018.4

Climate variable	Summary statistics for climate variables during wheat growing season						
NRW	Mean	STD	Minimum	25 %	50 %	75 %	Maximum
TempMin (°C)	4.4	0.9	2.8	3.9	4.3	5.1	6.3
TempMean (°C)	8.2	0.9	6.5	7.8	8.2	8.6	10.3
TempMax (°C)	12.1	0.9	10.3	11.8	12.2	12.5	14.3
Radiation (MJ m^{-2} d^{-1})	9.6	1.4	4.6	9.5	9.8	10.0	12.2
Windspeed (m s^{-1})	2.7	0.2	2.4	2.6	2.7	2.8	3.0
Precipitation (mm y^{-1})	632.0	151.4	194.0	587.5	674.8	692.3	801.0
ET$_0$ (mm y^{-1})	710.0	151.7	133.3	710.5	739.7	779.5	825.8
cwb (mm y^{-1})	78.0	106.7	-69.7	12.3	65.6	148.3	292.3
Tuscany	Mean	STD	Minimum	25 %	50 %	75 %	Maximum
TempMin (°C)	5.7	0.7	4.2	5.3	5.9	6.1	7.3
TempMean (°C)	12.5	0.8	10.6	11.9	12.6	12.8	14.2
TempMax (°C)	14.7	0.9	12.7	14.1	14.9	15.2	16.4
Radiation (MJ m^{-2} d^{-1})	11.9	1.9	5.3	11.8	12.1	12.6	14.4
Windspeed (m s^{-1})	2.1	0.2	1.8	2.0	2.1	2.2	2.4
Precipitation (mm y^{-1})	591.7	188.3	104.4	506.6	566.5	683.1	901.9
ET$_0$ (mm y^{-1})	697.9	164.6	83.5	696.1	739.8	768.0	810.5
cwb (mm y^{-1})	106.2	163.5	-252.5	10.6	89.4	255.7	358.0

894 *TempMin: Minimum Temperature, TempMean: Mean Temperature, TempMax: Maximum Temperature, ET$_0$: Reference

895 Evapotranspiration, cwb: Climate water balance (ET$_0$ − Precipitation) and others are as indicated

896 **Table 4. List of crop models used in the model ensemble**

No.	Model	Model abbreviation in text and figures	References
1	AgroC [b]	AGROC	6 (Herbst et al., 2008, Klosterhalfen et al., 2017)
2	Century	CENT	(Parton et al. 1992)
3	CoupModel [ab]	COUP	(Janssen 2012, Conrad and Fohrer, 2009)
4	DailyDayCent	DayC	(Del Grosso et al., 2001, 2006)
9	EPIC v. 0810	EPIC	(Williams 1995)
6	HERMES [b]	HERM	(Kersebaum, 2007, 2011)

7	MONICA [b]	MONI	(Nendel et al., 2011; Specka et al., 2015)
8	SIMPLACE<LINTUL5;SLIM>	LINT	(Gaiser et al., 2013; Shibu et al., 2010)
9	STICS	STIC	(Bergez et al., 2013; Brisson et al., 2009, 1998)

897 [a] only simulated wheat; [b] simulated NRW only

898 **Table 5. Crop management of winter wheat and silage maize in Tuscany.**

Management	Winter wheat	Silage maize	Unit	
Residues	cut and incorporated into soil	Cut and incorporated into soil	-	
Tillage	plough in late summer/beginning of autumn (harrowing in the plains)	plough in late summer/beginning of autumn (ripping in the plains)	-	
Sowing date	10-Nov	03-Apr	date	
Harvest date	25-Jun	03-Oct	date	
Plant density	400	8	m^{-2}	emerging plants
Sowing depth	3	3	cm	

899

900 **Table 6. Crop management of winter wheat and silage maize in NRW**

Management	Winter wheat	Silage maize	Unit	
Residues	straw is removed, stubbles are left on the field (10% of the above ground total biomass and the roots)	straw is removed, stubbles are left on the field (10% of the above ground total biomass and the roots)	-	
Tillage	ploughing in autumn	ploughing in autumn	-	
Sowing date	Oct-01	Apr-20	date	
Harvest date	Aug-01	Sep-20	date	
Plant density	400	10	$1/m^2$	emerging plants
Sowing depth	4	6	cm	

901

902 **Table 7. The abbreviation for input data combination of soil and climate data at different resolutions.**

*Soil resolution km	*Climate resolution km	SoilxClimate	Remarks
y	z	S_yxC_z	soil and climate aggregation
S_{Reg}	z	$S_{Reg}xC_z$	One dominant regional soil with climate aggregation
y	C_{Reg}	S_yxC_{Reg}	soil aggregation with average regional climate

903 * the subscripts y and z represents the resolution for soil and climate at 1, 10, 25, 50 and 100 km, S_{Reg} and C_{Reg}
904 are symbols to represents regional soil and climate (eg. S_{Tus} and C_{Tus} to represent for regional soil and regional
905 climate for Tuscany).

906

List of figure captions

Figure 1: Geographic location of the study regions and the elevation variability for NRW, (Germany) and Tuscany (Italy).

Figure 2: Soil type for NRW aggregated according to dominant soil types for resolutions from 1 km to 100 km (Hoffmann et al., 2016).

Figure 3: USDA soil texture class of the topsoil aggregated by dominant soil type from 1 km resolution.

Figure 4: Average minimum, mean and maximum temperature in Tuscany for the time period 1995-2013 at spatial resolutions from 1 km to 100 km

Figure 5: Sketch of the modelling framework used in this study. Combination of soil and climate data at different aggregation level are distributed to the model ensemble. The collected outputs of all models were averaged to obtain the model ensemble mean.

Figure 6: Ensemble mean crop yields for silage maize for NRW (A) and for Tuscany (B) under water-limited conditions for different levels of aggregation of soil and climate data. In each panel, the 1st row represents the ensemble mean yield for simultaneous aggregation of soil and climate data (S_yxC_z), 2nd row for aggregation of soil input data with the same regional mean climate data as S_yxC_{Reg} and 3rd row for the aggregation of climate data with regional dominant soil type as $S_{Reg}xC_z$.

Figure 7: Ensemble mean crop yields for winter wheat for NRW (A) and for Tuscany (B) for different levels of aggregation of soil and climate data. In each panel, the 1st row represent the ensemble mean yields for simultaneous aggregation of soil and climate input data (S_yxC_z), 2nd row for aggregation of soil with constant regional mean climate (S_yxC_{Reg}) and 3rd row aggregation of climate input data with regional dominant soil type as ($S_{Reg}xC_z$).

930   **Figure 8:** Average yield difference between coarser resolutions (S_yxC_z) and the reference

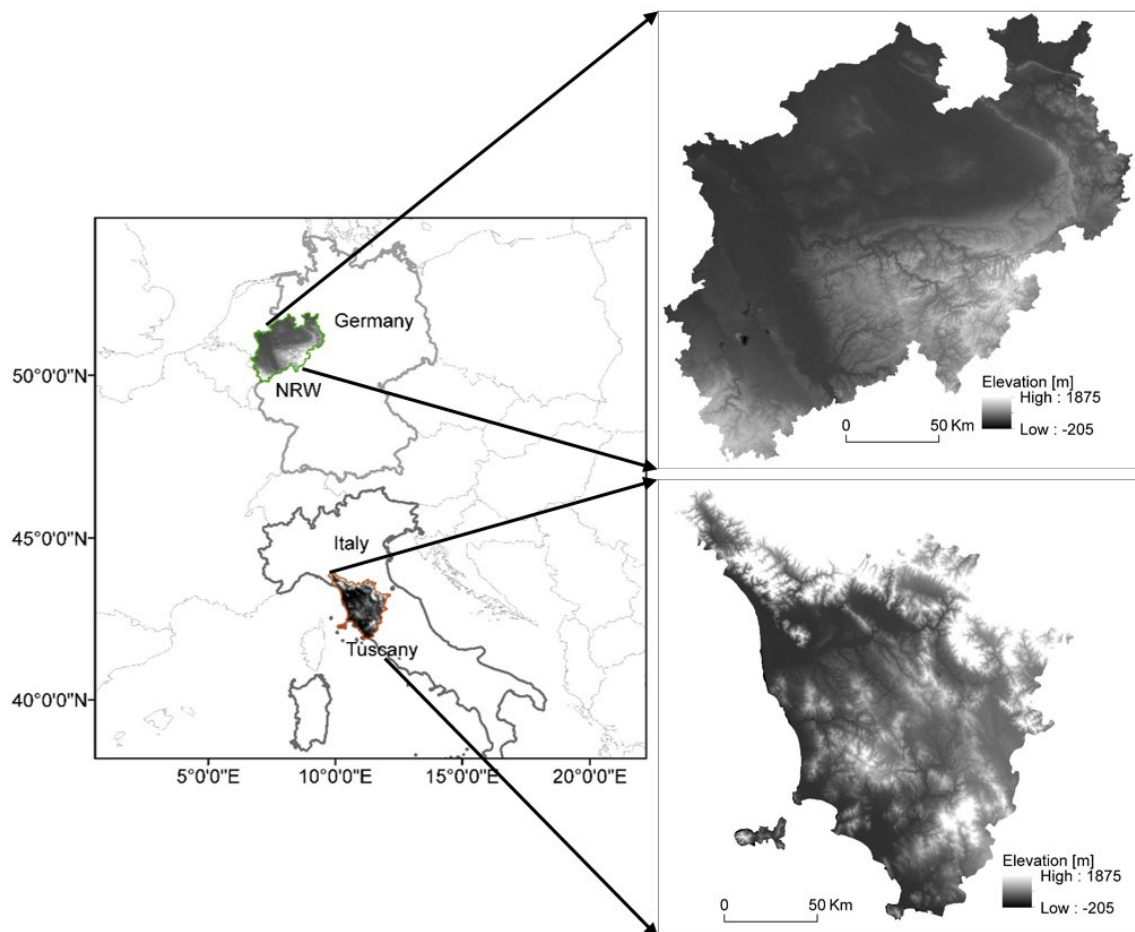931   resolution (S_1xC_1) for silage maize for NRW (A) and for Tuscany (B).

932   **Figure 9:** Percentage absolute difference for silage maize yields comparing coarser

933   resolutions (S_yxC_z) with the reference resolution (S_1xC_1) for NRW and Tuscany. The violin

934   plots (Hintze and Nelson, 1998) show in the x-dimension the distribution of the probability

935   density of the percentage in absolute yield difference values. The box plots show the median

936   (red line), mean (black star), and the upper and lower quartiles (box), as well as the extreme

937   upper and lower values (black lines)

938   **Figure 10:** The relative average absolute yield deviation (rAAD) as indicator for the impact

939   of soil and climate input data aggregation on silage maize yield simulations by different crop

940   models as well as for the model ensemble mean (ESMB)

941   **Figure 11:** Average yield difference between coarser resolutions (S_yxC_z) and the reference

942   resolution (S_1xC_1) for winter wheat for NRW (A) and winter wheat for Tuscany (B). AMD is
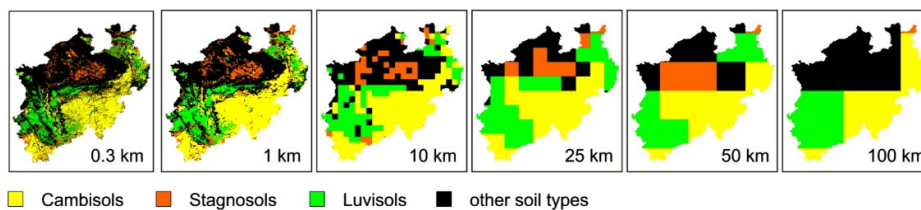
943   the average yield difference

944   **Figure 12:** Percentage absolute yield differences of winter wheat between coarser resolutions

945   (S_yxC_z) and the reference resolution (S_1xC_1) for NRW and Tuscany. The violin plots (Hintze

946   and Nelson, 1998) show in the x-dimension the distribution of the probability density of the

947   percentage in absolute yield difference values. The box plots show the median (red line),

948   mean (black star), and the upper and lower quartiles (box), as well as the extreme upper and

949   lower values (black lines)

950   **Figure 13:** The relative average absolute yield deviation (rAAD) as indicator for the impact

951   of soil and climate input data aggregation on winter wheat yield simulations by different crop

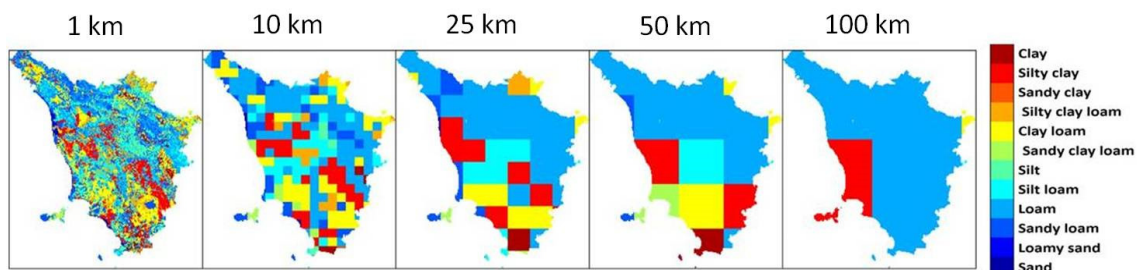952   models as well as for the model ensemble mean (ESMB).
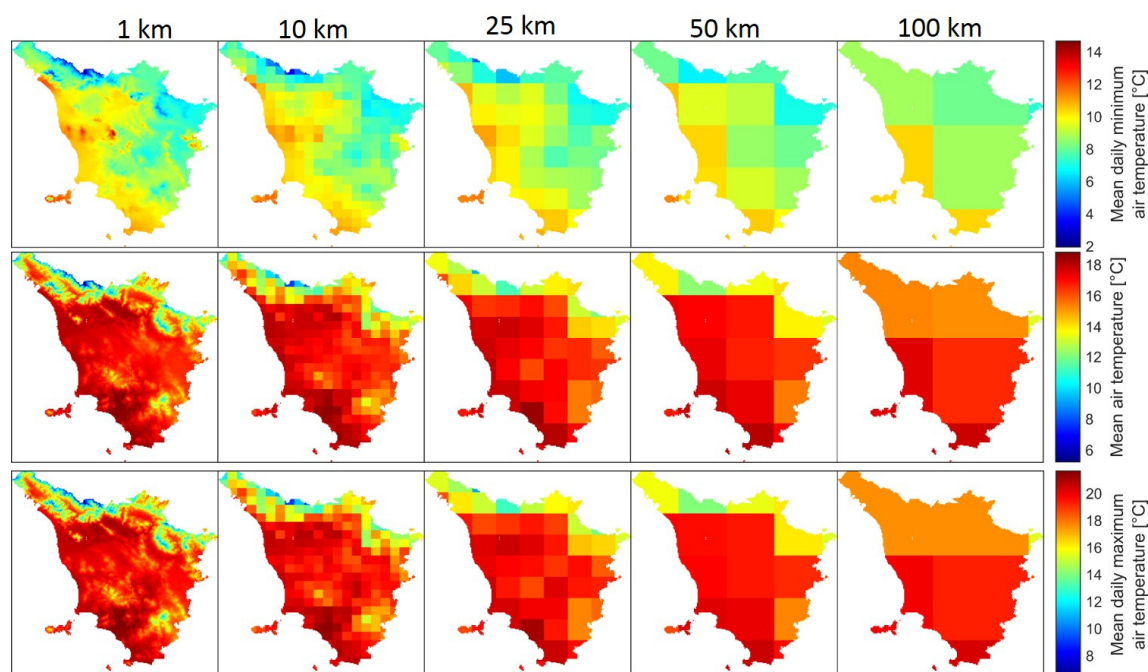
953

954

955   Figure 1

956   ☐ Cambisols   ☐ Stagnosols   ☐ Luvisols   ☐ other soil types

957   Figure 2

958

959   Figure 3

960

961   Figure 4

962

963   Figure 5

A

All average yield (Maize-PLW)
due to S_yxC_z combination by all_ESMB

S_1xC_1 S_{10}xC_{10} S_{25}xC_{25} S_{50}xC_{50} S_{100}xC_{100}

S_1xC_{NRW} S_{10}xC_{NRW} S_{25}xC_{NRW} S_{50}xC_{NRW} S_{100}xC_{NRW}

S_{NRW}x$C1$ S_{NRW}xC_{10} S_{NRW}xC_{25} S_{NRW}xC_{50} S_{NRW}xC_{100}

0.0 2.5 5.0 7.5 10.0 12.5 15.0 17.5 20.0 22.5 25.0
t ha^{-1}

B

All average yield (Maize-PLW)
due to S_yxC_z combination by NRR_ESMB

S_1xC_1 S_{10}xC_{10} S_{25}xC_{25} S_{50}xC_{50} S_{100}xC_{100}

S_1xC_{TUS} S_{10}xC_{TUS} S_{25}xC_{TUS} S_{50}xC_{TUS} S_{100}xC_{TUS}

S_{TUS}x$C1$ S_{TUS}xC_{10} S_{TUS}xC_{25} S_{TUS}xC_{50} S_{TUS}xC_{100}

0.0 2.5 5.0 7.5 10.0 12.5 15.0 17.5 20.0 22.5 25.0
t ha^{-1}

964

965   Figure 6

966

967

All average yield (Wheat-PLW)
due to $S_y \times C_z$ combination by all_ESMB

All average yield (Wheat-PLW)
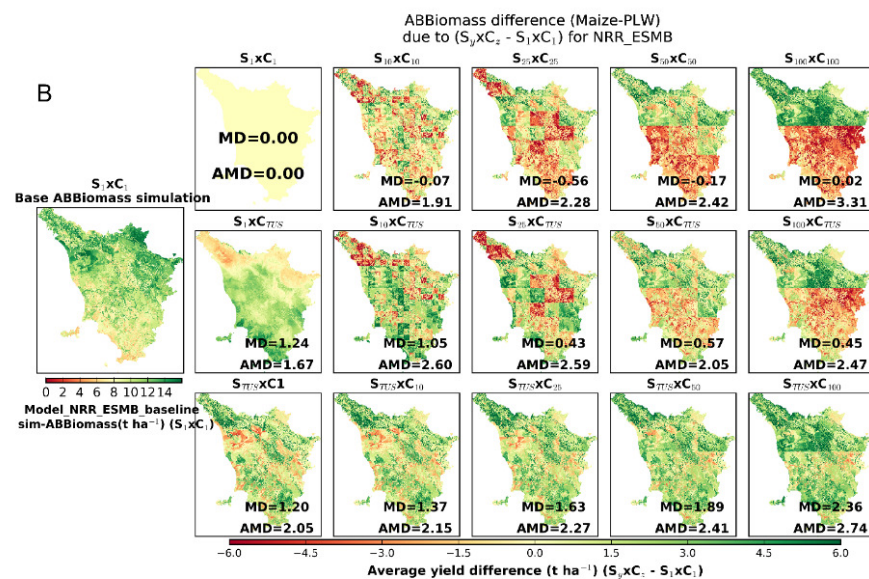due to $S_y \times C_z$ combination by NRR_ESMB

968

969   Figure 7

970

971

972

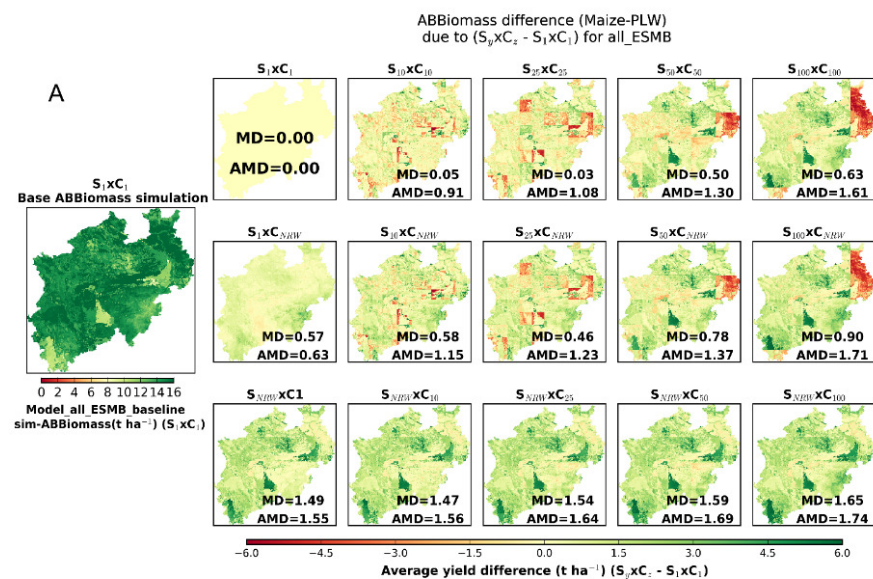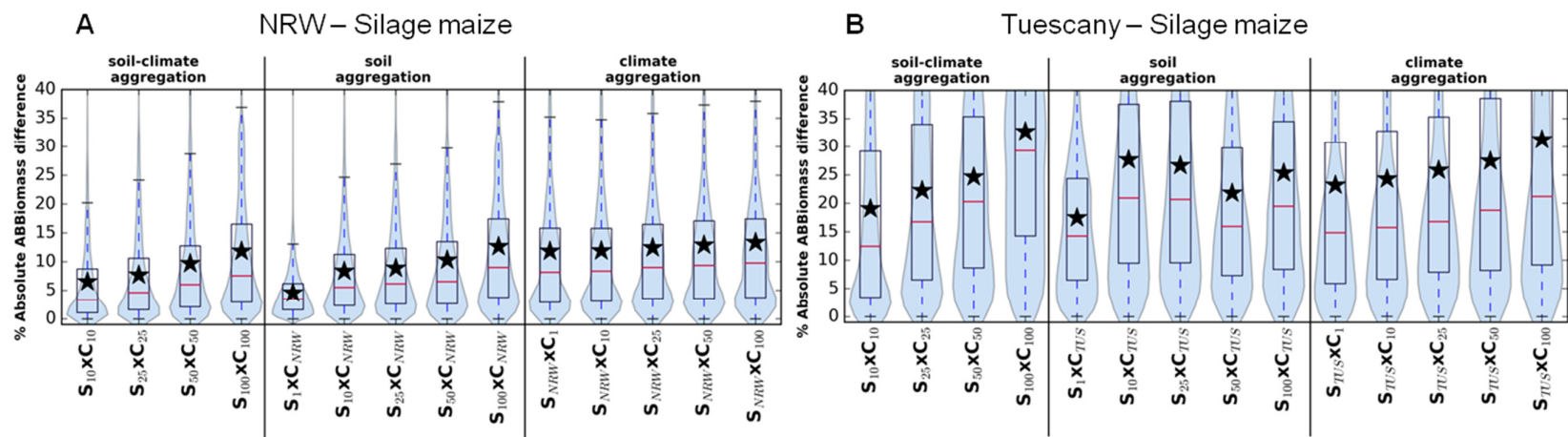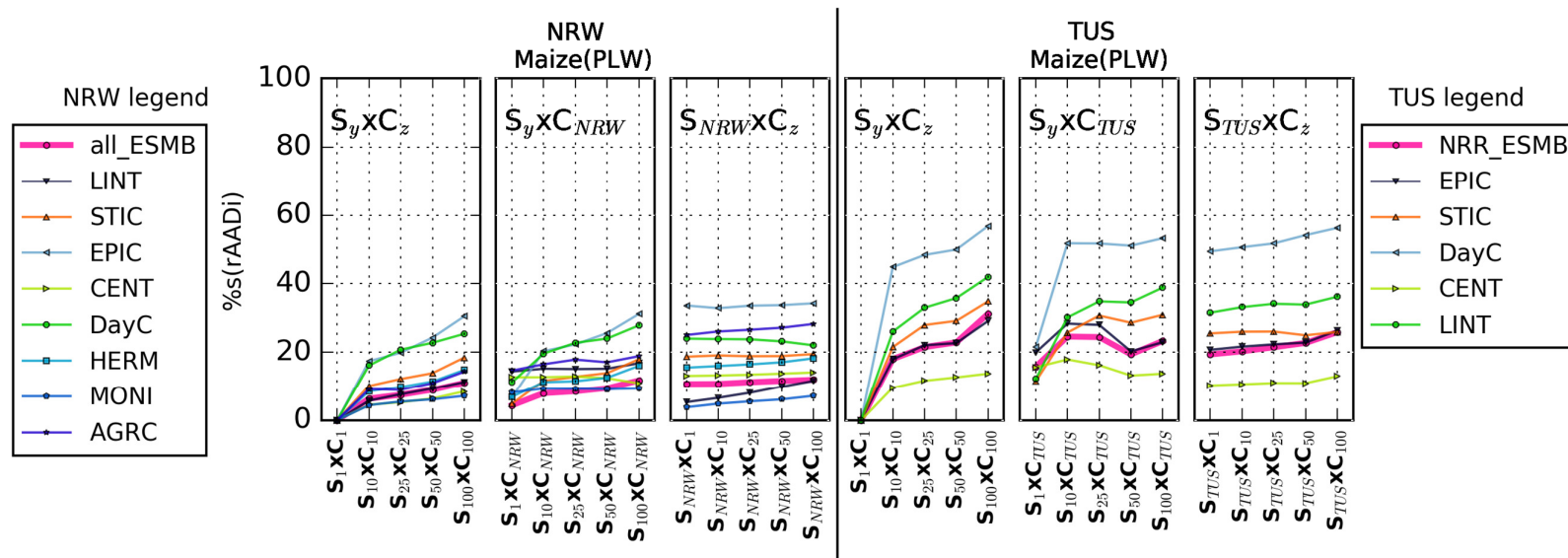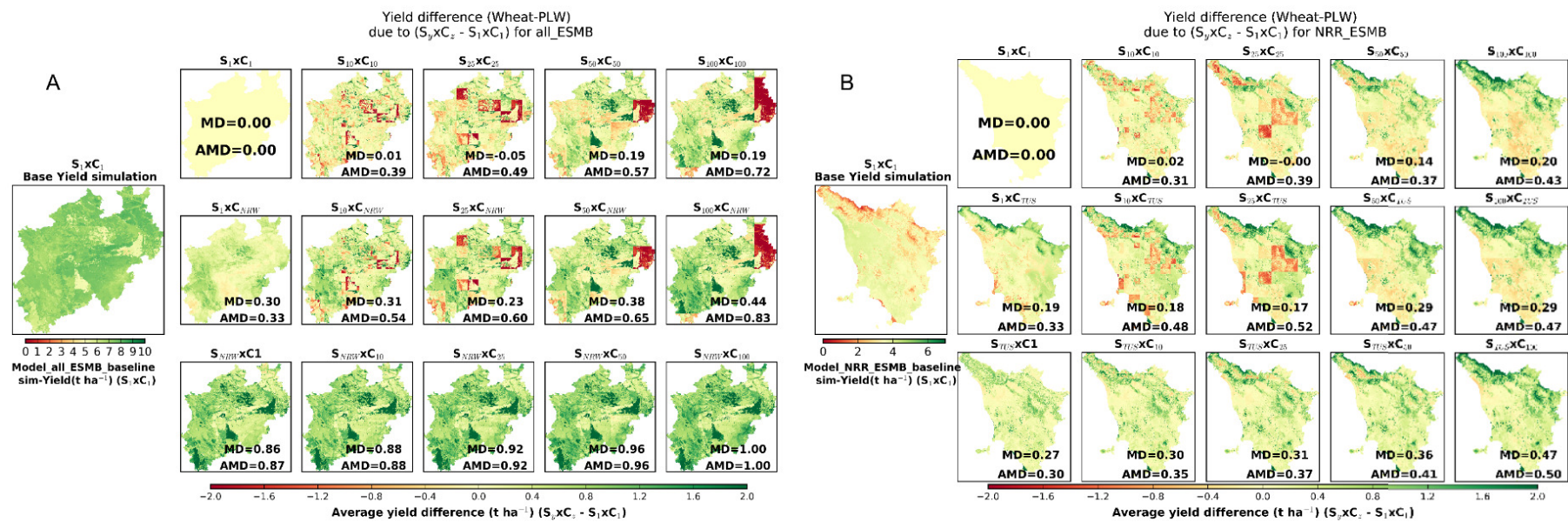973   Figure 8

974

975

976   Figure 9

977

978   Figure 10

979

980

981

982

Figure 11